Proceedings of the 2009 IEEE International Conference on Systems, Man, and Cybernetics
San Antonio, TX, USA - October 2009

Model Predictive Control of Velocity and Torque Split in a Parallel Hybrid Vehicle

Tae Soo Kim* , Chris Manzie and Rahul Sharma
Department of Mechanical Engineering
The University of Melbourne
Victoria, 3010 Australia
*t.kim2@pgrad.unimelb.edu.au

***Abstract*—Fuel economy of parallel hybrid electric vehicles is affected by both the torque split ratio and the vehicle velocity. To optimally schedule both variables, information about the surrounding traffic is necessary, but may be made available through telemetry. Consequently, in this paper, a nonlinear model predictive control algorithm is proposed for the vehicle control system to maximise fuel economy while satisfying constraints on battery state of charge, relative position and vehicle performance. Different scenarios are considered including allowing and disallowing overtaking; various hard and soft constraints; and computational aspects of the solution. The optimal control signal vector was found to be characterised by smooth changes in velocity and increases in the motor to engine power ratio as the vehicle accelerates. It was found that using feedforward information about traffic flow in the range of five to fifteen seconds has the potential for significant fuel savings over two urban drive cycles.**

***Index Terms*—Hybrid vehicle, Vehicle telematics, Model predictive control**

I. Introduction

With increasing market awareness for fuel efficient vehicles, automotive manufacturers are rapidly adopting various hybrid electric configurations (HEVs) to a wider range of passenger vehicles. Amongst all configurations the parallel hybrid electric vehicle, which allows either the internal combustion engine or the electric motor (or both) to deliver power to the wheels, is presently the choice for most OEMs. The different nature of the two power sources and the possibility of recouping kinetic energy via regenerative braking gives potential for extra fuel saving relative to a conventional vehicle.

The initial approaches to power split control strategies were based upon the heuristic knowledge on the characteristics of engine and motor. Rule-based [1] or fuzzy logic [2] schemes were typical, where a set of rules was used to divide the power requirement between the two sources. These control strategies helped early hybrid implementations, however did not fully exploit the potential fuel saving available.

A natural extension of the earlier approaches was the development of model-based control methods as a way to further push the envelope of fuel economy. The upper limit for fuel economy was established using dynamic programming over an entire known drive cycle to identify the globally optimal power split schedule [3]. This approach was useful in identifying the best possible fuel economy for a vehicle over a given drive cycle, however the technique is clearly infeasible to apply in real-world driving because the full knowledge of the drive cycle cannot be known *a priori* and there are considerable computational overheads with such approaches.

Later work focused on the real-time implementation of model-based control algorithms. The equivalent consumption minimisation strategy (ECMS) described in [4] and [5] attempted to minimise the overall fuel consumption online by instantaneously evaluating the fuel and electric energy use combined in a single cost. The equivalence factor, which equates the electric energy to the fuel equivalent energy, influenced the future charging/discharging behaviour of the battery to maintain its state of charge (SoC). An instantaneous optimisation can be applied online but the control performance was dependant upon the estimation of the equivalence factor which needed to be obtained offline for individual drive cycle.

With the idea of using vehicle telemetry in predicting the future traffic information, ECMS has been further improved by allowing the online estimation of the equivalence factor [6], thereby reducing the need to rely on static relationships between fuel and electrical energy in evaluating overall fuel efficiency. Meanwhile other research directions have focussed on exploiting the benefits of the traffic feedforward information. Using the limited preview of the velocity profile ahead as the receding horizon, model predictive control (MPC) approach was studied in [7]. In this work, the author employed a dynamic programming approach to solve for the power split in a HEV, since standard optimisation theory could not be implemented due to the nature of the vehicle model which was highly nonlinear and composed of both continuous and discrete inputs. Further work in this direction focussed on reducing the computational time of the dynamic programming algorithms employed in the MPC [8].

Consequently, the use of this information allows new strategies for fuel saving to be investigated, not just in scheduling the power split between the electric motor and the internal combustion engine but also through shaping the vehicle velocity profile to minimise fuel use and CO_2 emissions. A simple strategy explored [9] demonstrated that drive cycle smoothing using feedforward information can have significant impacts on the fuel efficiency of both hybrid and conventional powertrain vehicles. This work was extended in [10] and [11], where the additional possibilities in velocity shaping were considered in order to take advantage of the regenerative braking capability

978-1-4244-2794-9/09/$25.00 ©2009 IEEE

of HEVs.

This study attempts to build on the work in [10], using a model predictive control based approach to optimally schedule both torque split and vehicle velocity given a limited amount of traffic information. Model predictive control is a natural fit to this problem, given constraints on the internal states and system inputs, while the development of an appropriate cost function ensures that both the average vehicle velocity is unchanged and the battery state of charge is not depleted over the journey.

This paper considers two scenarios: one in which vehicle is allowed to overtake the lead vehicle while in the second case the vehicle position is restricted with no overtaking. It is demonstrated that in both scenarios significant improvement in fuel economy is achievable as the length of the preview increases.

II. Vehicle modelling

The hybrid vehicle is understandably a complex system that is composed of several highly nonlinear subsystems. Closed loop control of such a system must consider the constraints on states and inputs, as well as only limited feedforward information. Model predictive control is a natural fit for this problem, but direct implementation on high order models comes with a heavy computational burden, and consequently model reduction is necessary.

The reduced order model to be used in this work is characterised by backward flow of information form - i.e. the vehicle velocity is considered the input to the system and the fuel and electrical energy usage are the outputs. The reduced order model considers the total force demand for the vehicle as a function of velocity v

$$F_T(v) = F_D(v) + F_A(v) + F_R(v) \tag{1}$$

where F_D, F_A and F_R denote driving force, and the forces required to overcome aerodynamic drag and rolling resistance, respectively. The corresponding torque and speed at the wheel is obtained with the wheel radius.

Consequently, the torque and speed required at the torque coupler, T_{tc} and ω_{tc} respectively, are simple functions of the vehicle velocity, v, acceleration, Δv, and also the gear ratio, i:

$$\begin{bmatrix} T_{tc} \\ \omega_{tc} \end{bmatrix} = f_1(i, v, \Delta v) \tag{2}$$

The torque split ratio, u, specifies the proportion of the torque at the torque coupler which comes from the engine i.e.:

$$u = T_f / T_{tc} \tag{3}$$

The remaining fraction of the required torque, $1 - u$, is provided by the electric motor. When $u = 0$, all torque is provided by the electric motor only while $u = 1$ implies that only the engine is running. When $u > 1$, excess torque produced from engine will generate current to recharge the battery. The total power request at the torque coupler must meet the sum of the power from the engine, P_f, and motor, P_m, i.e.:

$$T_{tc}\omega_{tc} = T_f\omega_f + T_m\omega_m \tag{4}$$

With the torque and speed demand from the engine and motor, the fuel consumption, $\dot{m}_f$, and the electric power consumption may be calculated from experimentally obtained steady-state maps, $f_2(.)$ and $f_3(.)$

$$\dot{m}_f = f_2(T_f, \omega_f) \tag{5}$$

$$P_m = f_3(T_m, \omega_m) \tag{6}$$

The mass of fuel can be converted to an equivalent fuel power, P_f, and subsequently the experimentally obtained maps may be approximated by polynomials, $f_4(.)$ and $f_5(.)$

$$\hat{P}_f = f_4(i, v, \dot{v}, u) \tag{7}$$

$$\hat{P}_m = f_5(i, v, \dot{v}, u) \tag{8}$$

The electric energy request from the motor is supplied by the battery, under the assumption this is temperature independent. The open circuit voltage, V_{oc}, internal resistance, R_{int} and the electrical current, I are functions of battery state of charge, SoC. Thus the motor power demand can be expressed as:

$$P_e = V_{oc}(SoC)I(SoC, P_m, R_{int}(SoC)) \tag{9}$$

where the admissible range for SoC is between 0 and 1.

For a small change in the state of charge ($\pm$ 0.1 for the chosen battery model), a linear relationship exists between P_e and P_m which allows further simplification of the electric power consumption model.

$$\hat{P}_e = k_1\hat{P}_m + k_2 \tag{10}$$

Note the constants k_1 and k_2 are different for charging and discharging of the battery.

The rate of change of the state of charge is proportional to the electric power consumption.

$$\frac{d}{dt}\hat{SoC} = k_3\hat{P}_e \tag{11}$$

Lastly, a proportion of negative torque request at the wheel goes to regenerative braking and the rest is dissipated in the friction braking. As a further model simplification the proportion of the regenerative braking is assumed to be constant across all velocities during deceleration, i.e.:

$$T_{regen} = k_4 T_{wheel}, \qquad \text{when} \qquad T_{wheel} < 0 \tag{12}$$

III. Control Strategy

In this section, a control algorithm for the torque split and velocity of a parallel HEV with telemetry is proposed. This work extends the idea of the velocity algorithm of [9] using a model-based approach, by examining the set of nonlinear functions that approximate the vehicle fuel consumption, as presented in Section II. The outline of the formulation of the nonlinear MPC for torque split and velocity control follows. Note that the hybrid vehicle being controlled is denoted as *smart HEV* in this paper.

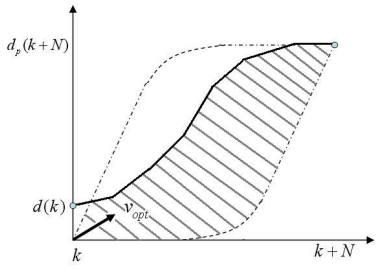

Fig. 1. Graphical representation of the position variation from the predicted velocity of lead vehicle (solid) and envelop of possible trajectories accounting for acceleration and velocity constraints (dashed).

A. Velocity trajectories

At time step k, the discrete velocity information of the traffic up to N time steps ahead of the smart HEV is assumed provided by telemetry :

$$\underline{v}_p = [v_{p|k}, v_{p|k+1}, ..., v_{p|k+N}] \tag{13}$$

The vehicle in front of the smart HEV is assumed to perfectly follow this velocity profile of the traffic, resulting in a set of future positions relative to the position of the smart HEV, $d_{p,k+N}$, given by piecewise integration of (13):

$$d_{p,k+N} = \sum_{j=k}^{k+N} v_{p|j} \triangle t + d_{p|k-1} \tag{14}$$

where $\triangle t$ is the velocity sampling time.

The lead vehicle velocity is the gradient of the solid curve in Figure 1. The smart vehicle control algorithm is responsible for selecting the velocity trajectory, $v_{c,i}$, based on this information.

$$\underline{v}_c = [v_{c|k}, v_{c|k+1}, ..., v_{c|k+N}] \tag{15}$$

Constraints on the velocity and acceleration clearly apply to each element of the trajectory in (15). Furthermore, a position constraint ensuring the same final position of the vehicle within the tolerance $\pm\delta$ can be set by integrating (15), i.e.:

$$d_{c,k+N} = \sum_{j=k}^{k+N} v_{c|j} \triangle t \leq d_{p,k+N} \pm \delta \tag{16}$$

If velocity is constrained only by the speed limits and/or vehicle performance limits, the envelope of trajectory is the dotted line in Figure 1. When the overtaking of the lead vehicle is disallowed, the trajectory must lie within the shaded region.

B. Cost Criteria

The formulation of the cost function requires the effects of vehicle velocity, battery state of charge and equivalent fuel energy of electrical use to be taken into consideration. Previous work, e.g. [4], defined a cost function to minimise the torque split control by the sum of the weighted cost of the fuel power and electric power at a particular instance in time.

$$J = \min_u (\hat{P}_f + s\hat{P}_e) \tag{17}$$

The key aspect of this equation is the weighting on the electric power usage, s, widely known as the equivalence factor. In this work, in order to fully utilise all feedforward information, the proposed cost function is the summation of the fuel and electric power consumption (weighted using the equivalence factor) over the prediction horizon N. The optimisation problem to be solved then becomes

$$\mathbf{u}^*, \mathbf{v}^* = argmin(\sum_{j=k}^{k+N} (\hat{P}_f(u(j), v(j), i_k) + s(k)\hat{P}_e(u(j), v(j), i_k)))$$

subject to

$$u \in [0, u_{max}], v \in [0, v_{max}], \dot{v} \in [-\dot{v}_{max}, \dot{v}_{max}] \tag{18}$$

where $\mathbf{u}^*$,$\mathbf{v}^* \in \Re^N$. Only the first values of $\mathbf{u}^*$,$\mathbf{v}^*$ are passed as the control inputs. i_k is the gear ratio at time step k and is assumed to be constant throughout the prediction horizon. The equivalence factor s is calculated in a similar way to Adaptive-ECMS [12], using the past and predicted velocity profiles over a limited window.

Two different ways of constraining the state of charge are proposed, to avoid excessive battery depletion during driving. The first approach is to include a hard constraint on the state of charge, where the value at the end of the prediction horizon is equal to that at the beginning of the journey. A small tolerance is permitted to aid feasibility of the solution to (18), ie:

$$SoC_{k+N} \in [SoC_{init} - \varepsilon, SoC_{init} + \varepsilon], \quad \varepsilon = 1\% \tag{19}$$

The second approach is to implement a soft constraint, where a penalty function is incorporated into the equivalence factor expression. This soft SoC contraint method was initially proposed in [11], [13], and the method here uses a linear penalty with weighting K to redefine the equivalence factor, s^*:

$$s^*(k) = s(k) + K(SoC - SoC_{init}) \tag{20}$$

The modified equivalence factor, s^*, is used in place of s in (18). The value of K must be tuned to bound the state of charge fluctuation within a desired level.

The traffic prediction is kept short, since the assumption on gear ratio and quality of information are not necessarily valid for a long prediction horizon where there are large changes in velocity. To solve (18), a Sequential Quadratic Programming (SQP) based optimisation algorithm in Matlab's *Optimization Toolbox* was implemented.

IV. Simulation Environment

All simulation results are obtained using the vehicle simulation software package ADVISOR. The overall schematic of the vehicle is depicted in Figure 2, where the shaded blocks represent the standard parallel hybrid powertrain and the unshaded blocks are the telemetry and controller where the optimal torque split and velocity are computed. The flow of

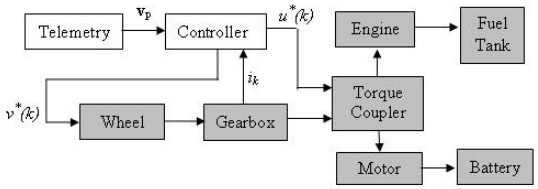

Fig. 2. Schematic of HEV configuration with telemetry and controller

information in the simulation is in the direction of the arrows. Thus, given the vehicle velocity demand, the corresponding fuel use and battery power use are returned.

The specification of the parallel HEV is chosen to the power requirements of a conventional family size sedan, with 95kW maximum power output engine, 75kW motor and the battery of 25Ah capacity. Other standard characteristics of parallel HEV are considered, including the engine shuts off when the vehicle is stationary, and the clutch disengages the engine from the torque coupler when the torque request to the engine is below zero.

The drive cycles chosen for the simulation are the NEDC and US-FTP cycles. As these prescribed drive cycles include no road grade information there is no need to take this into account, although previous work (e.g. [7] and [8]) indicate this may be important.

V. Results

A. Comparison of hard and soft constraints on state of charge

To investigate the use of the soft and hard constraints on the SoC while ensuring the constraints are satisfied, each case was simulated on a small section of the NEDC drive cycle with a short prediction horizon of 5 seconds. Optimisation tolerance on the control variables was set to 0.5 to improve the speed of computation. The results are plotted in Figure 3.

It is apparent that the use of a hard constraint on the state of charge results in non-smooth trajectories in vehicle velocity - most obviously during the period of 120 to 150 seconds. This result is unphysical, and most likely due to the SQP optimisation terminating once the algorithm's tolerance is met. Reducing the tolerance severely increases the time required to find the solution to (18) at each time step, and is thus not considered appropriate at this time.

When soft SoC constraints of the form described in (20) are used, the smart vehicle exhibits a smoother velocity profile. This is clearly a more 'feasible' solution, was faster and resulted in slightly lower use in fuel over the interval compared to the use of hard constraints, indicating optimality of the solution is not adversely impacted. Consequently, soft constraints were adopted for the remainder of the work.

B. Simulation results over NEDC and US-FTP cycles

Figure 4 shows the simulation through the entire NEDC drive cycle with a five second prediction horizon with overtaking of the lead vehicle allowed. The SoC variation is plotted together with smart velocity and torque split out of the

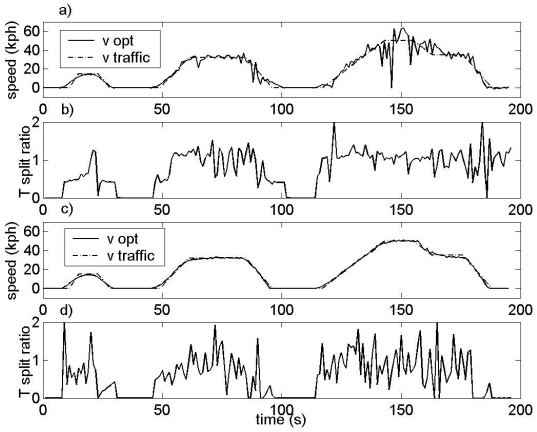

Fig. 3. Smart HEV velocity and torque split with 5 second prediction horizon. Hard SoC constraint (a and b) vs soft SoC constraint (c and d)

controller. While the velocity is relatively smooth in the earlier part of the cycle, a high frequency chattering-like behaviour is observed at higher speed region, which caused excessive use of energy, causing sudden drop in the SoC. The similar high frequency behaviour is also present for the torque splits, as shown in Figure 4 b), which is clearly undesirable in practice due to engine wear and vibrations from heavy switching. This phenomenon is due to increasing the optimisation tolerance settings, which was unavoidable due to the heavy computational demand especially when the prediction horizon is lengthened.

To reduce the high frequencies, two different methods are considered. The first method is to add hard constraints on $\triangle u$ and $\triangle v$ to (18). However this method of constraining the variables significantly increases the computational time.

An alternative approach to remove the high frequency components of the control signals is including a low-pass filter (LPF) on the output of the controller. The simulation result through the NEDC drive cycle with low-pass filter is shown in Figure 5. It is clear in Figure 5 b) that the low-pass filter has effectively eliminated the high frequencies present in the torque split control signal, and with the soft constraint on state of charge with $K = 150$ it effectively bound SoC fluctuation within 3% of the initial SoC. Simulation results over the US-FTP cycle with a low-pass filter are presented in Figure 6.

C. Varying traffic preview length

Figure 7 and 8 demonstrate the velocity and torque split ratio for two different preview lengths, five and 15 second. Note that only subsection of the total drive cycle is shown to highlight the effect of changing preview lengh. Figure 7 a) and c) show that, as the length of the preview becomes longer, the vehicle tends to start earlier than the front vehicle. One of the two interesting observations is that the velocity becomes smoother with longer preview, which is similar behaviour to [9] where a very simple averaging approach was used to set

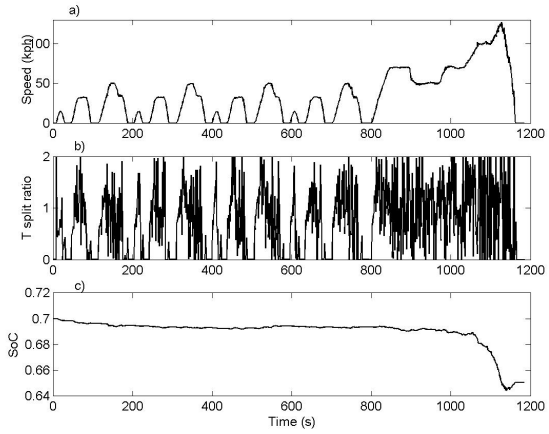

Fig. 4. Result with 5 second traffic preview on full NEDC cycle without LPF. Smart velocity (a), torque split ratio (b), SoC variation(c)

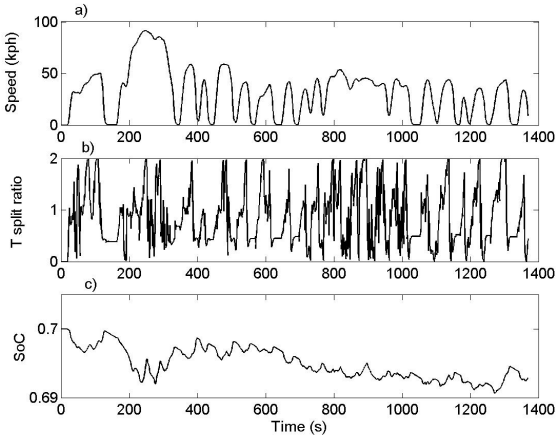

Fig. 6. Result with 5 second traffic preview on full US-FTP cycle with LPF. Smart velocity (a), torque split ratio (b), SoC variation(c)

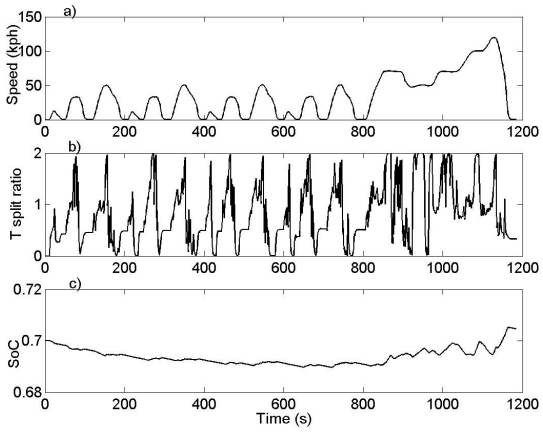

Fig. 5. Result with 5 second traffic preview on full NEDC cycle with LPF. Smart velocity (a), torque split ratio (b), SoC variation(c)

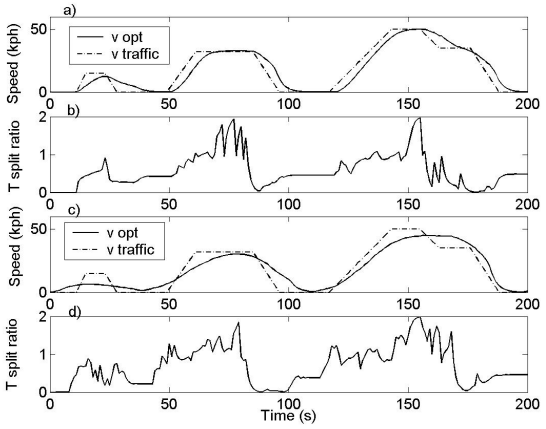

Fig. 7. Smart HEV speed and torque split with (a and b) 5 second and (c and d) 15 second prediction horizons using NEDC cycle.

the vehicle velocity.

The corresponding torque splits are shown in Figure 7 b) and d). The two figures show that the torque split ratio stays close to zero at low speeds, implying greater use of the electric energy. This phenomenon coincides with the standard result that the electric motor is more efficient for producing high torque at low speeds.

In Figure 9 a) the separation between the smart HEV and the lead vehicle is plotted. It is apparent that the smart vehicle switches its relative position to the front vehicle by either leading or lagging throughout a journey, and with longer traffic preview the range of separation becomes larger. This is mainly due to the fact that the vehicle uses the feedforward information to begin moving sooner and decelerates slightly later. While this behaviour may be feasible on a multiple lane road, it may require either delaying the acceleration of the smart HEV, or incorporating positional constraints into the solution of (18).

A numerical comparison of the total equivalent fuel energy consumption over the NEDC and US-FTP cycle is summarised in Table I and Table II. Torque split control and torque split and velocity control for prediction horizon from 0 to 15 seconds are listed and the percentage improvements are shown with respect to the rule-based torque split controller. By controlling the torque split only in a HEV with prediction horizon, the percentage of fuel consumption improvement stays between $1.1 - 2.5\%$. This agrees with the findings in [8] where it was shown that with DP based MPC algorithm for torque split control for routes with flat topographic profile could only achieve $0.5 - 2\%$ fuel saving in comparison with a non-predictive controller. On the other hand, scheduling the velocity as well can significantly improve fuel energy savings. With as short as five second traffic preview, the controller achieved 3.5% and 6.6% savings on the US-FTP and NEDC

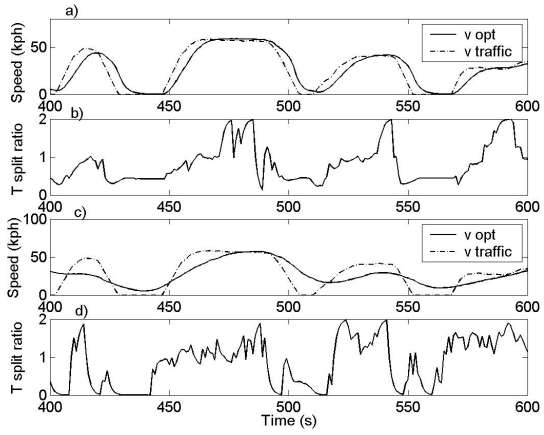

Fig. 8. Smart HEV speed and torque split with (a and b) 5 second and (c and d) 15 second prediction horizons using US-FTP cycle.

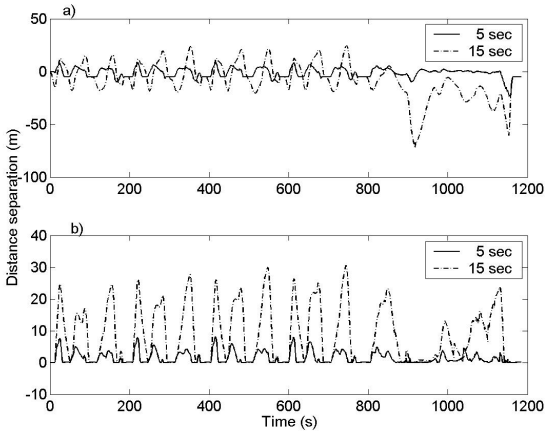

Fig. 9. Smart HEV distance separation from the front vehicle with varying prediction horizon length. overtaking allowed (a), overtaking not allowed (b)

cycles, and these improve further with increasing prediction horizon.

TABLE I
NUMERICAL COMPARISON OF THE FUEL ECONOMY, NEDC CYCLE

Preview (s)	Controlling u only (%)	Controlling u and v (%)	Controlling u and v with overtaking constraint(%)
rule-based	9.64 (-)	-	-
0	9.53 (1.1)	9.53 (1.1)	-
5	9.46 (1.9)	9.01 (6.6)	9.28 (3.7)
10	9.44 (2.1)	8.92 (7.5)	9.19 (4.7)
15	9.43 (2.2)	8.85 (8.2)	9.00 (6.6)

D. Incorporation of overtaking constraint

Overtaking of the lead vehicle is not feasible when the vehicle is traveling on a single-laned road or in heavy traffic.

TABLE II
NUMERICAL COMPARISON OF THE FUEL ECONOMY, US-FTP CYCLE

Preview (s)	Controlling u only (%)	Controlling u and v (%)	Controlling u and v with overtaking constraint(%)
rule-based	8.91(-)	-	-
0	8.75 (1.9)	8.75 (1.9)	-
5	8.74 (2.0)	8.60 (3.5)	8.72 (2.1)
10	8.71 (2.4)	8.47 (4.9)	8.59 (3.6)
15	8.70 (2.5)	8.35 (6.3)	8.49 (4.7)

The simulations on NEDC and US-FTP cycles are repeated with an explicit position constraint enforcing the smart vehicle remains behind the lead vehicle, as discussed in Section III-A. Figure 9 b) is the plot of vehicle separation between smart HEV and the lead vehicle with no overtaking condition. The separation remains positive indicating constraint satisfaction (c.f. Figure 9 a)). The fuel consumptions for this case are tabulated in the last column of Table I and Table II and demonstrate that even with the position constraints, significant fuel saving is achievable in comparison to torque split control only.

REFERENCES

[1] N. Jalil, N. Kheir, and M. Salman, "Rule-based energy management strategy for a series hybrid vehicle," in *American Control Conference*, 1997.

[2] N. Schouten, M. Salman, and N. Kheir, "Fuzzy logic control for parallel hybrid vehicles," *IEEE Transactions on Control Systems Technology*, vol. 10, p. 460, 2002.

[3] F. Kirschbaum, M. Back, and M. Hart, "Determination of the fuel-optimal trajectory for a vehicle along a known drive cycle," in *15th Triennial World Congress of the International Federation of Automatic Control*, 2002.

[4] G. Paganelli, S. Delprat, T. Guerra, J. Rimaux, and J. Santin, "Equivalent consumption minimization strategy for parallel hybrid powertrains," in *Vehicular Technology Coference*, 2002.

[5] A. Sciarretta, M. Back, and L. Guzzella, "Optimal control of parallel hybrid electric vehicles," *IEEE Transactions on Control Systems Technology*, vol. 12, no. 3, pp. 352–363, 2004.

[6] A. Sciarretta and L. Guzzella, "Control of hybrid electric vehicles," *IEEE Control System Magazine*, pp. 60–70, 2007.

[7] M. Back, S. Terwen, and V. Krebs, "Predictive powertrain control for hybrid electric vehicles," in *IFAC Symposium on Advances in Automotive Control*, 2004.

[8] L. Johannesson and B. Egardt, "A novel algorithm for predictive control of parallel hybrid powertrains based on dynamic programming," in *Fifth IFAC Symposium on Advances in Automotive Control*, 2007.

[9] C. Manzie, H. Watson, and S. Halgamuge, "Fuel economy improvements for urban driving: Hybrid vs. intelligent vehicles," *Transportation Research Part C*, vol. 15, pp. 1–16, 2007.

[10] T. Kim, C. Manzie, and H. Watson, "Fuel economy benefits of look-ahead capability in a mild hybrid configuration," in *IFAC World Cogress 08*, July 2008.

[11] T. van Keulen, B. de Jager, A. Serrarens, and M. Steinbuch, "Optimal energy management in hybrid electric trucks route information," in *IFP Conference on Advances in Hybrid Powertrains*, November 2008.

[12] C. Musardo and G. Rizzoni, "A-ecms: An adaptive algorithm for hybrid electric vehicle energy management," in *IEEE Conference on Decision and Control*, December 2005.

[13] J. Liu and H. Peng, "Modeling and control of a power-split hybrid vehicle," *IEEE Transactions on Control Systems Technology*, vol. 16, no. 6, pp. 1242–1251, 2008.